Teleoperation of a Robot Manipulator Using a Vision-Based Human–Robot Interface

Jonathan Kofman, *Member, IEEE*, Xianghai Wu, Timothy J. Luu, and Siddharth Verma

***Abstract*—Remote teleoperation of a robot manipulator by a human operator is often necessary in unstructured dynamic environments when human presence at the robot site is undesirable. Mechanical and other contacting interfaces used in teleoperation require unnatural human motions for object manipulation tasks or they may hinder human motion. Previous vision-based approaches have used only a few degrees of freedom for hand motion and have required hand motions that are unnatural for object manipulation tasks. This paper presents a noncontacting vision-based method of robot teleoperation that allows a human operator to communicate simultaneous six-degree-of-freedom motion tasks to a robot manipulator by having the operator perform the three-dimensional human hand–arm motion that would naturally be used to complete an object manipulation task. A vision-based human–robot interface is used for communication of human motion to the robot and for feedback of the robot motion and environment to the human operator. Teleoperation under operator position control was performed with high accuracy in object placement on a target. Semi-autonomous traded and shared control using robot-vision guidance aided in achieving a more accurate positioning and orientation of the end-effector for object gripping tasks.**

***Index Terms*—Human–robot interface, real time, robot manipulator, semi-autonomous control, teleoperation, traded and shared control, vision-based tracking.**

I. Introduction

ADVANCES in computer vision have led to increased complexity of tasks that can be carried out by fully autonomous robots. However, in highly unstructured dynamic environments, where objects are unfamiliar, changing shape, or moving with unknown motion, and for complex tasks, human intelligence is needed in the decision making and control of the robot, especially in delicate and dangerous environments. When human presence at the robot site is undesirable or difficult, remote human teleoperation of the robot is required. Such cases include handling hazardous materials, dismantling bombs, mines, or nuclear facilities, and operating in inaccessible sites in rescue, undersea exploration, and mining.

Commonly used mechanical human–machine interfaces for teleoperation, include a variety of devices worn by an operator, such as exoskeletal mechanical devices [1], instrumented gloves [2], [3], electromagnetic [4] or inertial [4], [5] motion tracking sensors, or electromyographic muscular activity sensors [6]. However, these contacting devices may hinder dexterous human motion due to the presence of the devices, sensors or attached cables. Other contacting interfaces, such as mechanical robot-arm replicas, dials, joysticks, computer mouse, and computer graphical interfaces [7], require operator motions that may be unnatural and must be learned. Vision-based interfaces employing hand gestures [8] have been developed and used with speech recognition, to allow a more intuitive and natural command to be given by the operator, without the constraints of physical devices. However, these interfaces are used at the level of distinct commands for separate simple robot tasks, such as positioning and orientating the end-effector and grasping, and often as a series of smaller tasks, such as translating up or down, rotating, pausing, continuing and changing mode of operation. These interfaces would be difficult to operate when the required complexity of robot manipulator motion is high. Single-camera tracking of hand motion has been used in robot teleoperation [9] and in teleoperation simulation [10]. However, motion commands are limited to a subset of the actual end-effector degrees of freedom. Furthermore, hand motions unrelated to the specific object manipulation task are required to change robot operating modes [9], thus making the communication of the manipulation task unnatural. Ideally, a natural means of communicating complex tasks to a robot manipulator without having to break up the task into limited commands allowed by the human–robot system and without the limitations of contacting physical devices, sensors and wires, is desired.

This paper presents a method of robot teleoperation that allows a human operator to communicate simultaneous motion tasks to a robot manipulator by having the operator perform the three-dimensional (3-D) human hand–arm motion that would naturally be used to complete an object manipulation task. The presented method of robot manipulator teleoperation uses a noncontacting vision-based human–robot interface for both the communication of the human motion to the robot and for feedback of the robot motion and interaction with objects in its environment to the human operator. The vision-based interface allows the human to perform hand and arm motions without the physical constraints of cables connected to sensors, contacting sensors and mechanical devices. The operator is able to concentrate on the task at hand, rather than on how to break

Manuscript received March 1, 2004; revised August 16, 2004. Abstract published on the Internet July 15, 2005. This work was supported by the Natural Sciences and Engineering Research Council of Canada (NSERC) through research and equipment grants.

J. Kofman was with the Department of Mechanical Engineering, University of Ottawa, Ottawa, ON K1N 6N5, Canada. He is now with the Department of Systems Design Engineering, University of Waterloo, Waterloo, ON N2L 3G1, Canada, (e-mail: jkofman@engmail.uwaterloo.ca).

X. Wu was with the University of Ottawa, Ottawa, ON K1N 6N5, Canada. He is now with the Department of Systems Design Engineering, University of Waterloo, Waterloo, ON N2L 3G1, Canada (e-mail: xianghaiwu@yahoo.com).

T. J. Luu was with the University of Ottawa, Ottawa, ON K1N 6N5, Canada. He is now with the Department of Mechanical and Aerospace Engineering, Carleton University, Ottawa, ON K1S 5B6, Canada (e-mail: timluu@gmail.com).

S. Verma was with the University of Ottawa, Ottawa, ON K1N 6N5, Canada. He is now with the Department of Mechanical Engineering, McGill University, Montréal, QC H3A 2K6, Canada (e-mail: sidd_verma@yahoo.com).

Digital Object Identifier 10.1109/TIE.2005.855696

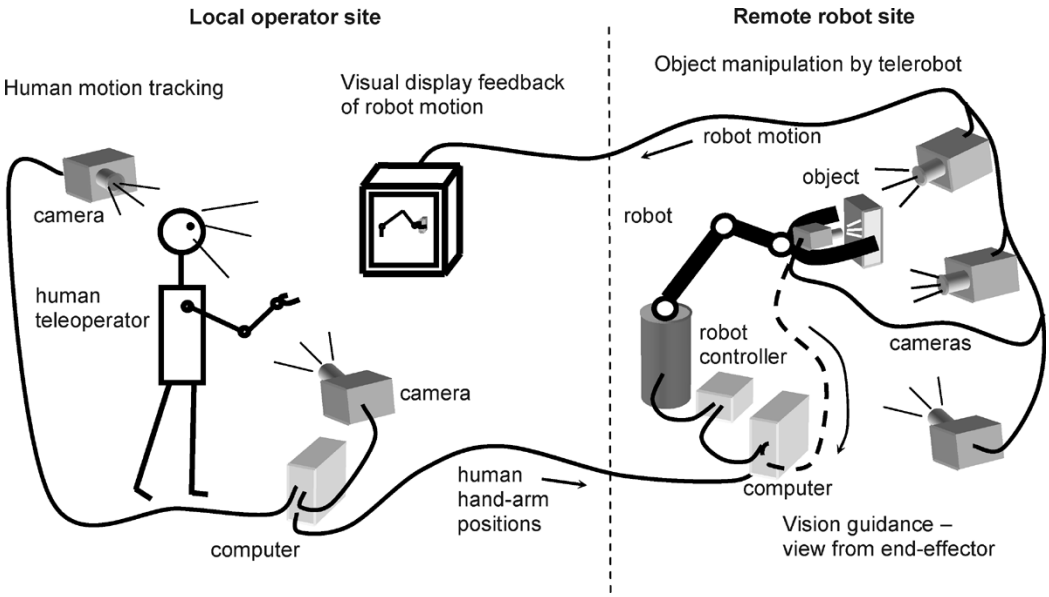

Fig. 1. Schematic representation of the human–robot-manipulator interface used for robot teleoperation showing local operator site and remote robot site, and four systems for: human motion tracking, object manipulation by telerobot, visual display feedback, and end-effector vision guidance.

the task into limited commands that the human–robot system understands for each type of robot motion.

Robot-manipulator teleoperation is carried out using position control, whereby the 3-D human-operator hand and arm motion is tracked by stereo cameras and the reconstructed 3-D hand–arm motion is used to control the position and orientation of the robot manipulator end-effector in real time. Indirect visual feedback of the robot interaction with objects in its environment is provided to the human operator. A description of the human–robot-manipulator interface is given in Section II. The human tracking and robot-motion feedback systems are described in Sections III and IV, respectively. Robot position control is carried out using direct control under full operator control, as well as semi-autonomous traded and shared control using a vision-guidance system. These control methods are detailed in Section V. This is followed by robot-teleoperation experiments in Section VI, results and discussion in Sections VII and VIII, respectively, and concluding remarks in Section IX.

II. Human–Robot-Manipulator Interface

The vision-based human–robot interface was developed for teleoperation of a six-axis robot manipulator at the Human-Machine Interfaces and Intelligent Systems Laboratory, University of Ottawa, Ottawa, ON, Canada. The interface consists of four main systems, shown schematically in Fig. 1.

1) A stereo-camera-based human-motion tracking system is used to track the human hand–arm motion and obtain two-dimensional (2-D) image coordinates of the hand and arm of the human operator at the local operator site. The 2-D hand–arm positions are sent to a remote robot-site computer for 3-D reconstruction in the local-site stereo-camera coordinate system, based on a stereo-camera calibration performed at the local-operator site.
2) A six-axis robot manipulator coupled to a robot controller at the remote robot site is used to perform object manipulation tasks. A remote-site computer receives 2-D human hand–arm position information from the human-tracking system, and performs 3-D reconstruction of the position and orientation of the hand to control the robot via the robot controller. Communication between the local operator-site and remote robot-site computers is performed over a local area network.
3) A visual display feedback system is composed of cameras at the remote robot site to obtain continuous images of the robot interacting with objects in its environment, and a television monitor at the local operator site to provide visual feedback of the robot environment to the human operator.
4) A vision-guidance system consists of a camera mounted on the robot end-effector, a frame grabber, and computer at the remote-robot site to acquire and process images from the robot end-effector viewpoint.

During robot-manipulator teleoperation, the human operator performs hand–arm motions that would naturally be used to complete an object manipulation task. Information of the human hand–arm positions is acquired by the human-motion tracking system at the local operator site and sent to the remote site computer. The remote-site computer processes the human position information and controls the robot to copy the human motion at the remote site via the robot controller. Images of the robot motion are obtained by cameras at the remote site and are sent to the local site for visual feedback to the human operator to aid them in controlling the robot. This human teleoperation of the robot is carried out in real time. The vision-guidance system at the remote robot-site uses images from the robot end-effector-mounted camera to guide the robot end-effector motion via the robot controller. This is performed using semi-autonomous control described further in Section V.

III. Human Hand–Arm Tracking

Tracking of the human operator hand–arm motion at the local operator site is carried out using a stereo-camera system

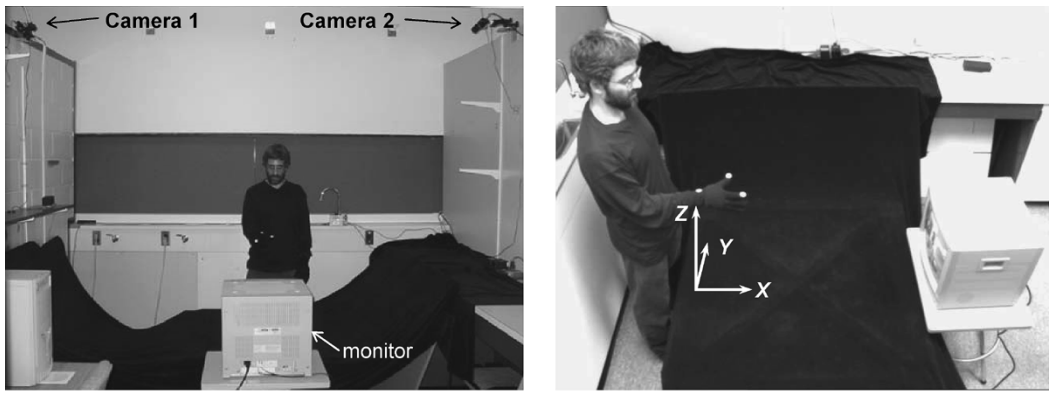

Fig. 2. Local operator site showing (a) two overhead cameras used for tracking human-operator hand–arm motion and (b) view from Camera 1 for tracking wrist, thumb, and index-finger markers on teleoperator hand. The monitor for visual feedback of the robot site is also shown.

consisting of two Watec WAT-902H monochrome cameras (Watec America Corporation) with 1/2-in CCD and 570 TV-line resolution, a Matrox Meteor-II PCI multichannel frame grabber, and a Pentium IV 1.6–GHz processor—256 MB RAM computer. The local site for human-operator tracking is shown with the two overhead cameras and the human operator facing the visual feedback monitor in Fig. 2(a). The operator wears a black glove on the hand with a white circular marker placed at each of the following locations: on the radial side of the wrist, at the end of the thumb on the dorsal side, and at the end of the index finger on the radial side, such that the three markers are visible in the two overhead cameras views. The view from Camera 1 is shown in Fig. 2(b). The operator is clothed on the upper body and hands in black, and a black cloth is used for the background, to facilitate identification of the white markers in the camera images. Before marker tracking begins, the three markers on the wrist, thumb, and index finger, respectively, are labeled in an image from each camera. During tracking for robot teleoperation, the stereo-camera system acquires an image of the human hand and arm from each of the two cameras, and the 2-D image coordinates of the centroids of the three markers are computed and sent to the robot-site computer over a local area network in real time. To enable marker tracking and coordinate data transmission in real time, the automatic tracking algorithm uses the marker positions from the previous frame to minimize the search for the new marker positions in each new frame.

The 3-D coordinates of the hand markers are reconstructed in the operator-site stereo-camera coordinate system in real-time by the remote-site Pentium IV 1.8 GHz computer, from the 2-D marker-position information sent from the local-operator-site computer. The X, Y and Z coordinates of each of the wrist, thumb, and index finger markers are computed for every image frame using calibration parameters determined earlier by stereo-camera calibration using the Direct Linear Transformation (DLT) [11]. The calibration was performed using a working volume of approximately 1 m $\times$ 1 m $\times$ 1 m for the human-operator hand motion.

The 3-D position of the wrist-marker centroid on the hand of the operator is used to control the position of the robot-manipulator end-effector. This is explained in further detail in Section V-A. The orientation of the hand of the operator is used to control the orientation of the robot-manipulator end-effector and is computed from the 3-D coordinates of the centroids of the three hand markers as shown in Fig. 3. Firstly, the midpoint of the line segment joining the thumb and index-finger marker centroids, T and I, respectively, is defined as M (Fig. 3(a)). A coordinate system $X_0Y_0Z_0$ with origin at wrist W is then defined by a translation of the local-site global reference coordinate system XYZ to the wrist [Fig. 3(b)]. Through yaw, pitch, and roll rotations, explained below, the final axes $X_3Y_3Z_3$ to be used to determine the tool axes of the robot-end-effector are obtained with X_3 collinear with $\overline{WM}$, WTI coplanar with X_3Y_3, and T lying in the first quadrant of X_3Y_3, as shown in Fig. 3(b).

The yaw–pitch–roll tool rotation angles are determined directly from the hand rotation angles of $\overline{WM}$ and $\overline{TI}$ as follows: yaw rotation α of coordinate system $X_0Y_0Z_0$ about Z_0 to $X_1Y_1Z_1$, pitch rotation β of $X_1Y_1Z_1$ about Y_1 to $X_2Y_2Z_2$, shown in Fig. 3(c) using $-\beta$ for clarity, and roll rotation γ of $X_2Y_2Z_2$ about X_2 to $X_3Y_3Z_3$, as shown in Fig. 3(d). The angles are computed as follows:

$$\alpha = \tan^{-1}\left(\frac{M_{0y}}{M_{0x}}\right) \tag{1}$$

$$\beta = \tan^{-1}\left(\frac{M_{0z}}{\sqrt{M_{0x}^2 + M_{0y}^2}}\right) \tag{2}$$

$$\gamma = \tan^{-1}\left(\frac{I_{2z} - T_{2z}}{I_{2y} - T_{2y}}\right) \tag{3}$$

where $I_0(x,y,z) = [I_{0x}, I_{0y}, I_{0z}]^\top$, $T_0(x,y,z) = [T_{0x}, T_{0y}, T_{0z}]^\top$, and $M_0(x,y,z) = [M_{0x}, M_{0y}, M_{0z}]^\top$ are the 3-D coordinates of I, T, and M, with respect to $X_0Y_0Z_0$, respectively; and $I_2(x,y,z) = [I_{2x}, I_{2y}, I_{2z}]^\top$ and $T_2(x,y,z) = [T_{2x}, T_{2y}, T_{2z}]^\top$ are the 3-D coordinates of I and T, with respect to $X_2Y_2Z_2$, respectively,

$$I_2(x,y,z) = R_{Y_1}^{-1}(-\beta)R_{Z_0}^{-1}(\alpha)I_0(x,y,z) \tag{4}$$

$$T_2(x,y,z) = R_{Y_1}^{-1}(-\beta)R_{Z_0}^{-1}(\alpha)T_0(x,y,z) \tag{5}$$

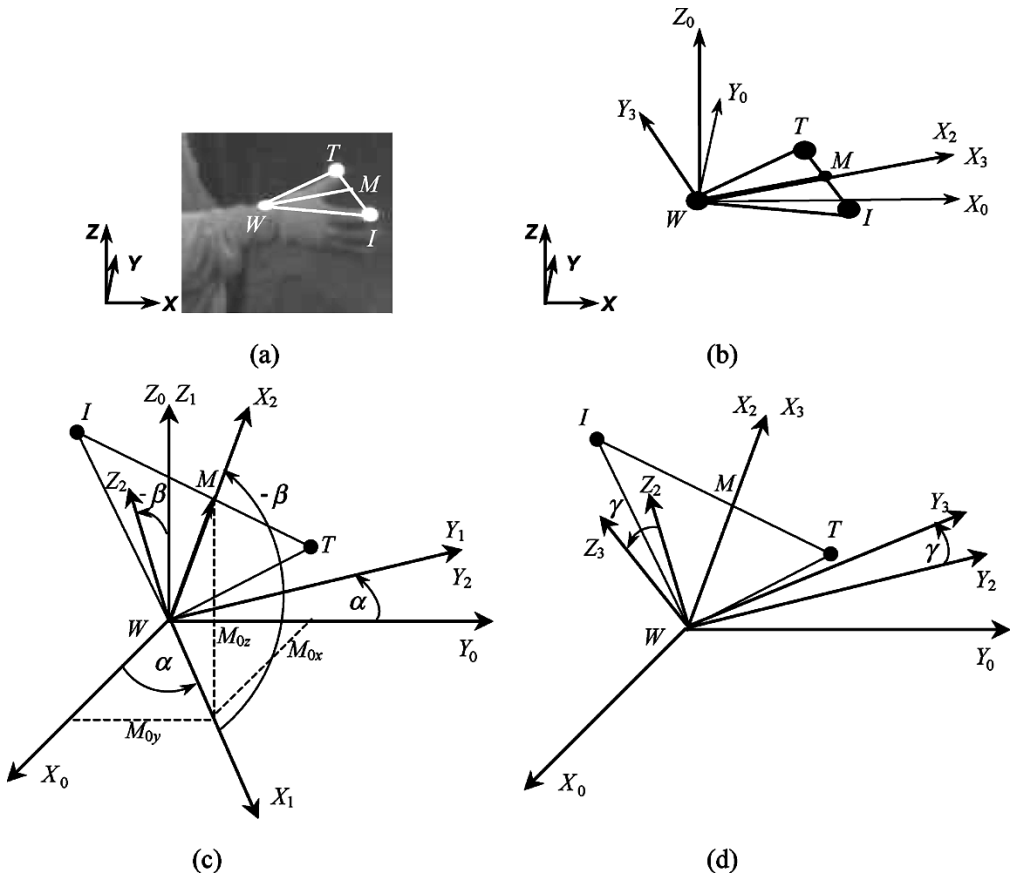

Fig. 3. Determination of tool orientation from hand-orientation angles using (a) hand-marker centroids: thumb, T; wrist, W; and index-finger, I on hand, and computed midpoint M between T and I. (b) Local-site global reference system XYZ translated to wrist to obtain $X_0Y_0Z_0$ with origin at wrist W and final axes $X_3Y_3Z_3$ rotated by yaw, pitch, roll, to obtain X_3 collinear with $\overline{WM}$, WTI coplanar with X_3Y_3, and T in first quadrant of X_3Y_3. (c) Determination of yaw α and pitch β angles. (d) Determination of roll γ angle.

where $R_{Z_0}(\alpha)$ is the rotation matrix about the Z_0 axis

$$R_{Z_0}(\alpha) = \begin{bmatrix} \cos\alpha & -\sin\alpha & 0 \\ \sin\alpha & \cos\alpha & 0 \\ 0 & 0 & 1 \end{bmatrix} \tag{6}$$

and $R_{Y_1}(-\beta)$ is the rotation matrix about the Y_1 axis

$$R_{Y_1}(-\beta) = \begin{bmatrix} \cos(-\beta) & 0 & \sin(-\beta) \\ 0 & 1 & 0 \\ -\sin(-\beta) & 0 & \cos(-\beta) \end{bmatrix}. \tag{7}$$

IV. Robot-Motion Feedback to Human Operator

During teleoperation of the robot manipulator, indirect visual feedback of the robot environment is provided to the human operator by the visual display feedback system. The system employs four cameras at the remote robot site, as shown in Fig. 4(a), to obtain continuous images of the robot interacting with objects in its environment, and a television monitor at the local operator site to provide simultaneous display of the four camera views, as shown in Fig. 4(b). The feedback display monitor is positioned in front of the human operator to enable the operator to view their own arm at the same time as the views of the remote robot site, as shown in Fig. 2(a) and (b). This visual feedback of the arm position was found useful in preliminary teleoperation trials. Cameras 1 and 3 are positioned facing the robot from the front at 0.5 m from the robot end-effector in its starting position, along the X axis, at 565 mm above and 35 mm below the robot end-effector starting position, respectively [Fig. 4(a)]. Camera 2 is located 1.05 m to the right of the robot and directed parallel to the Y axis. Camera 4 is mounted on the robot end-effector midway between the gripper fingers, and is tilted downward to provide a view of an object and the gripper finger ends. The view of Camera 4 is also shown when approaching an object in Fig. 4(c). This view facilitates alignment and positioning of the end-effector by the human operator for object gripping. This view is also used in the semi-autonomous vision guidance system used in semi-autonomous traded and shared control of the robot manipulator, discussed in Section V-B.

V. Robot-Manipulator Control

The method of teleoperation using the vision-based interface was developed using a six-axis Thermo CRS A465 robot manipulator equipped with a Thermo CRS two-finger servo-gripper end-effector (Fig. 5). Three methods of controlling the robot manipulator are used: direct, traded, and shared control. Direct position control is carried out with the operator hand as the master and the robot end-effector as the slave, with indirect visual feedback from the robot environment to the operator as described in Section IV. To facilitate grasping of objects, a combination of semi-autonomous traded control using the vision-guidance

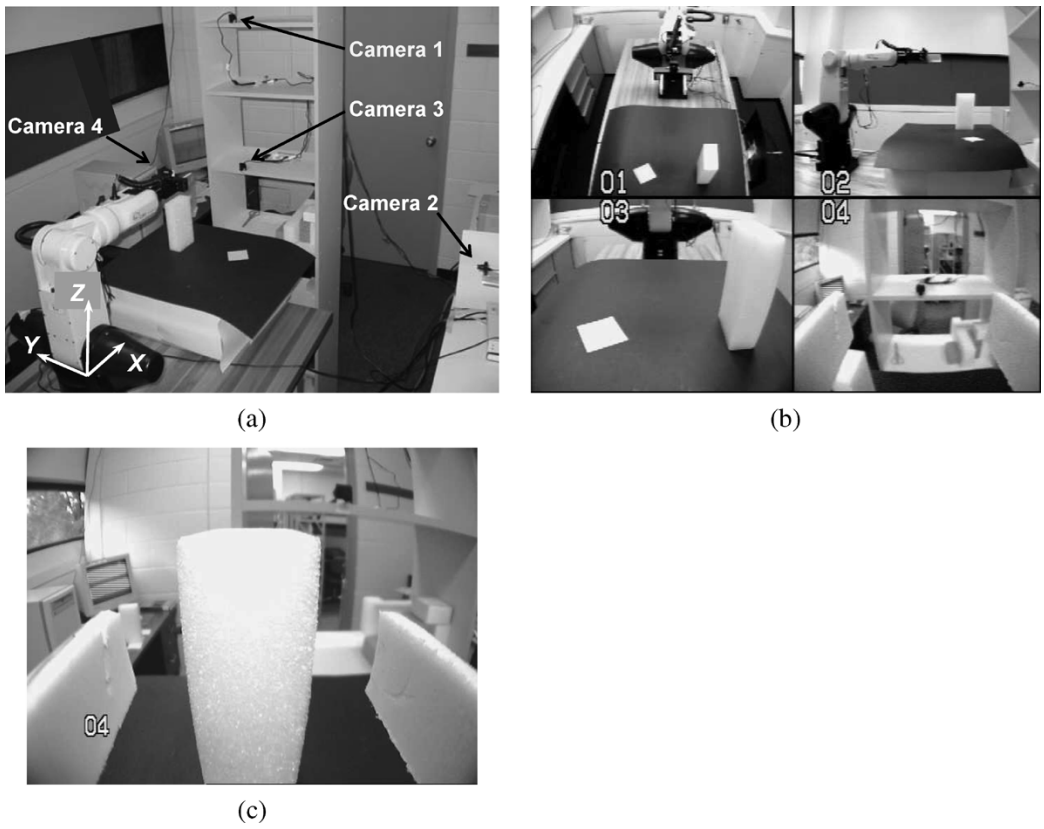

Fig. 4. Robot-motion feedback system showing (a) remote robot site with robot and four cameras to obtain images of the robot environment, (b) simultaneous display of the four cameras views for indirect visual feedback of the remote-robot site to the human teleoperator, and (c) view of Camera 4 when approaching an object for an object gripping task.

system and shared control are used together with indirect visual feedback from the robot environment to the operator. The control methods are described in the following sections.

A. Direct Robot-Manipulator Control

Direct position control is carried out with the operator hand as master and the robot end-effector as slave. Relative motion of the three markers on the master hand of the human operator, one on each of the wrist, thumb, and index finger, from their starting positions shown in Fig. 2(b), are used to control the relative motion of the robot end-effector from its starting position shown in Fig. 5(b) and (c). To initialize the human–robot-manipulator interface, the hand is placed in the starting position approximately centered in the calibrated control volume along Y and toward the rear of the volume [Fig. 2(b)]. The 3-D positions of the thumb, index-finger, and wrist markers in the global stereo-camera coordinate system at the local operator site are stored as reference teleoperator positions T^0, I^0, and W^0, respectively. From the initial 3-D position of the three markers, the initial orientation of the hand, given by the yaw, pitch, and roll angles α, β, and γ, respectively, are computed as described in Section III. The initial position and orientation of the robot end-effector in the starting position [Fig. 5(b) and (c)] are also stored as reference positions and orientations.

During teleoperation, the 3-D hand-marker positions are reconstructed by the robot-site computer from the 2-D marker positions, received from the local operator site computer using a local area network. Under the assumption that the human operator hand motion is slow, outlier positions that yield a motion from the previous position beyond a predetermined threshold are ignored. The 3-D marker positions are then filtered by a normalized one-sided Gaussian low-pass filter using the current and previous marker positions. This effectively smoothes the 3-D marker positions with the highest weighting on the current and most recent positions and decreasing weighting on earlier positions as follows:

$$P^k = \frac{\sum_{i=0}^{n-1}\left(\frac{1}{\sigma\sqrt{2\pi}}e^{\frac{-(\Delta t)i^2}{2\sigma^2}}\right)P'^{k-i}}{\sum_{i=0}^{n-1}\left(\frac{1}{\sigma\sqrt{2\pi}}e^{\frac{-(\Delta t)i^2}{2\sigma^2}}\right)} \tag{8}$$

where P^k is the general marker current position after filtering, for either the thumb T^k, index-finger I^k, or wrist W^k; and k is the index of the current position. P'^{k-i}, $i = 0, 1, 2, \ldots n-1$ are the raw marker positions before filtering, for a history of n image frames, i is the index for the position history beginning at $i = 0$ for the current position and $i = 1$ for the previous position, Δt is the sampling period in seconds, which was 0.2 s, and σ is the standard deviation, which was set to 3.0. The number of image frames, n, which is effectively the filter window width, was set to 5.

The positions of the hand markers following filtering, T^k, I^k, and W^k, are then used to compute the relative motions of the human-hand markers from their initial positions in the

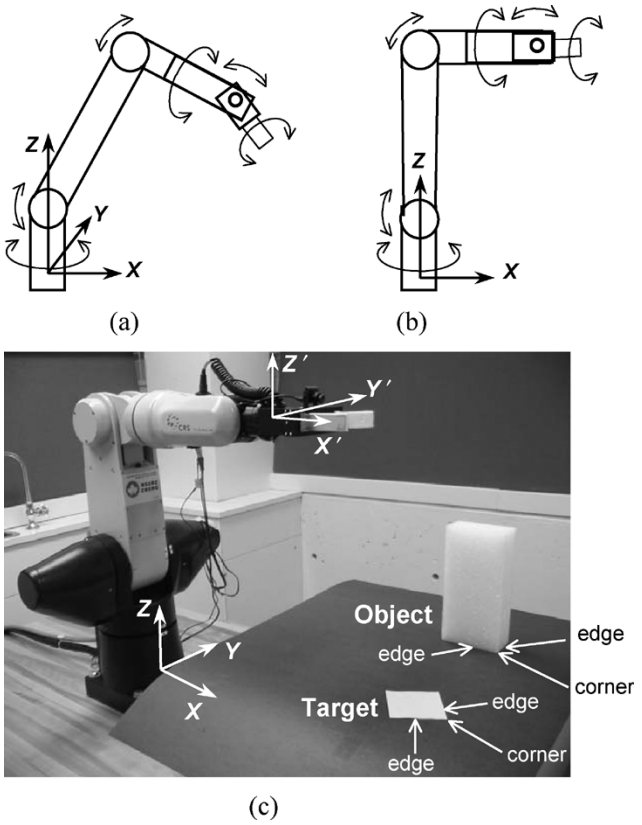

Fig. 5. Six-axis robot manipulator used at the remote robot site. (a) Schematic representation showing six degrees of freedom. (b) Schematic representation showing degrees of freedom and starting position. (c) Robot manipulator in the experimental setup at the remote robot site in the starting position, showing the object starting position and the specified object and target corner locations. The robot global coordinate axes XYZ and robot tool coordinate axes $X'Y'Z'$ are shown.

stereo-camera coordinate system, T^0, I^0, and W^0, by: $T^k - T^0$, $I^k - I^0$, and $W^k - W^0$, for every image frame k. The relative wrist position, $W^k - W^0$, is applied as a relative motion of the robot end-effector tool-control point from its initial position in the robot global-coordinate system. Similarly, the relative orientations of the hand from the initial hand orientations in the stereo-camera coordinate system are computed using the filtered hand-marker positions and the yaw, pitch, and roll angles defined in Section III (Fig. 3). The relative hand orientations are applied as relative rotations of the end-effector from its initial orientation in the robot tool-coordinate system, shown in Fig. 5(c).

For gripping tasks, such as picking up and releasing objects, the operator can naturally communicate commands to open and close the gripper by opening and closing their fingers in a pinch grip. The two-finger servo gripper is sent a command to close when the distance between the human thumb and index-finger markers is less than a preset threshold τ_1

$$\|T^k - I^k\| < \tau_1. \tag{9}$$

The closing of the gripper is carried out under force control by the servo-gripper using a small percentage of the maximum allowable gripping force, in order to prevent crushing of an object. A gripper opening command is executed when the distance between the thumb and index-finger markers is greater than a second threshold τ_2

$$\|T^k - I^k\| > \tau_2 \tag{10}$$

where $\tau_2 > \tau_1$. The thresholds τ_1 and τ_2 were set to 70 and 100 mm, respectively. This hysteresis technique using two separate thresholds allows the human operator to relax their hand after performing a gripper closing without causing an unintentional gripper opening. It also accommodates any residual noise in the thumb and index-finger marker positions. A repeated sequence of hand closing and opening within a predefined period is used in transferring control between the operator and robot as explained in Section V-B.

All commands to the Thermo CRS six-axis robot are made via the Thermo CRS robot controller from user-written C++ programs that are run on the remote-site computer and employ CRS Active Robot software functions.

B. Semi-Autonomous Traded and Shared Robot-Manipulator Control

1) Traded and Shared Control: To facilitate grasping of an object, semi-autonomous traded and shared control approaches can be used, whereby the human–robot interface employs a vision system to control robot motion for part of a robot end-effector positioning task. Traded control allows the operator to hand over control to the robot and take it back again, while shared control allows the operator and robot to share some level of control. In some approaches, structured light has been used to obtain information of the shape and orientation of an object for robot end-effector path guidance [12]. In this paper, a single-camera view from the end-effector-mounted camera is used for vision guidance in teleoperated grasping of an object under traded and shared control.

The vision-guided teleoperated grasping of an object is carried out as follows. Beginning with traded control, the operator first performs coarse positioning of the end-effector near the object. The operator then closes and opens their hand twice within a short predefined period to transfer control to the robot. The robot vision guidance system is then used to perform fine alignment and centering of the gripper with the object, using tool-roll rotation about X' and translation in Y'. Any motion of the operator's hand is ignored during this period; however, the operator is permitted to take back full control of the end-effector motion by performing a transfer-control command using a close–open–close–open sequence with their hand. Once the alignment and centering are completed, the human–robot interface uses shared control. Under shared control, the operator only controls motion of the end effector toward or away from the object along the robot tool axis X' while the robot controls motion in the other end-effector degrees of freedom: Y', Z', yaw α, pitch β, and roll γ. The operator may also perform a closing of the gripper on the object, or take back full control by a quick close–open sequence. If the operator performs a close gripper command, the operator continues to be allowed control of end-effector motion only along the tool axis X'. This would most likely be used to take the object. After a predefined time

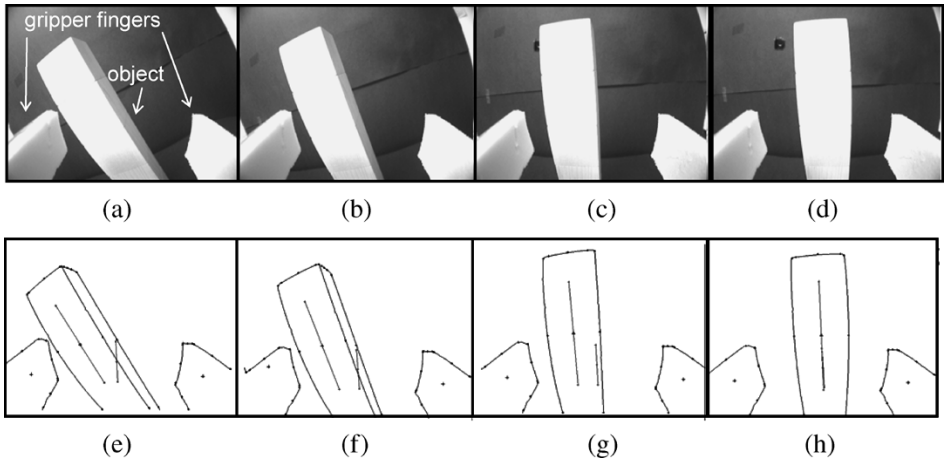

Fig. 6. Views of object and gripper fingers from the end-effector-mounted camera, Camera 4, during semi-autonomous gripper alignment and centering. (a)–(d) Raw images and (e)–(h) processed images showing edge detection, and object and gripper midlines. The initial misalignment of the robot gripper fingers with the object is shown in (a) and (e), intermediate positions of the gripper during alignment and centering using the robot-site vision-guidance system are shown in (b), (c), (f), and (g), and successful alignment and centering of the robot gripper with the object is shown in (d) and (h).

period, set to 5 s, full control is returned to the operator, so that they may place the object in a new location.

2) Vision-Guided Robot End-Effector Fine Alignment and Centering: Vision-guided end-effector fine alignment and centering is carried out by first performing Canny edge detection by the remote-robot-site computer on continuously acquired images from the end-effector-mounted camera, Camera 4 (Fig. 4). Images of an end-effector alignment and centering sequence are shown in Fig. 6, with raw images in Fig. 6(a)–(d), and processed images in Fig. 6(e)–(h). The corners of the gripper fingers are pre-identified and located in the image before the start of the robot teleoperation. The corner positions would remain the same throughout robot teleoperation for the fully open gripper. The midline between the gripper fingers is located as shown in the processed images. As well, the medial line of the object between the longest two parallel edges is computed. The orientation of the end-effector is first adjusted by a roll rotation about the tool axis X', to minimize the angle between the gripper-fingers midline and object medial line. This is followed by the centering by end-effector translation along the Y' tool axis, to minimize the distance between the two lines. Finally, higher resolution adjustment of both orientation and centering are performed.

3) Human Adaptive Control: Several human-adaptive characteristics have been included in the human–robot system. Under shared control, the human–robot interface adapts to the skill level and dexterity of the human operator. In preparing to grasp an object under shared control, adaptation is done by adjusting the gripper fine positioning and alignment step size and thus adjusting the speed of position and alignment correction. This is performed based on the error in position and alignment achieved by the operator in coarse positioning the end-effector near the object. Also, in semi-autonomous control, once the vision-guided positioning and alignment of the end-effector with the object is completed by the robot-vision system, the speed of approach and retreat of the end-effector normally controlled by the operator hand motion, is dynamically adjusted to compensate for the operator approaching the object too quickly, which could risk collision. The robot thus adapts to poor operator control.

VI. Robot Teleoperation Experiments

Tests were carried out to evaluate the ability of the vision-based human–robot-manipulator interface to permit a human operator to perform object manipulation tasks in real time using the remote robot manipulator. Essentially the tests were evaluating both the ability of the robot manipulator to copy human hand–arm motions, and the ability of the user to use the human-robot-manipulator interface. One type of experiment was carried out to test the use of direct position control and a second type of experiment used two series of tests to study the semi-autonomous traded and shared control with vision-guided end-effector alignment and centering.

In the first type of experiment, a series of ten repeated object manipulation tasks was carried out with the operator having full direct position control of the robot end-effector, and thus without use of the robot-site vision-guidance system. Beginning with the robot in the starting position, as shown in Fig. 5(b) and (c), the task was to pick up an object from a starting position and place a specified object corner at a specified target corner location on a predetermined target with predefined object and target edges aligned [Fig. 5(c)]. The object was a rigid plastic foam block, 203 mm in height, 100 mm wide, and 49 mm thick. The starting position of the object was 80 mm from the front tip of the gripper in the robot starting position in X, and 130 mm in Y, on a base board 360 mm below the gripper, as shown in Fig. 5(c), and in the camera views in Fig. 4(b). The target was a square (76.5 mm $\times$ 76.5 mm) paper, rotated 45° and placed approximately 260 mm in the $-Y$ direction from the object starting position, with the specified object and target corners as shown in Fig. 5(c). All six degrees of freedom of the robot were used and the test was repeated ten times. After the object was placed on the target, the position and orientation of the object relative to the target were recorded to determine the accuracy in placing the object on the target. Positioning errors were determined by

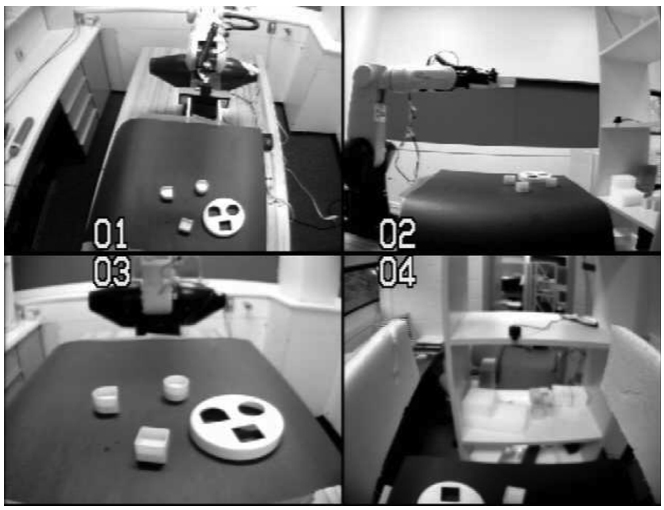

Fig. 7. Four robot-site camera views of the robot manipulator, the extruded-shape objects (circle, square, and modified square) and target with three corresponding holes, in their starting positions for the experiment in peg-in-hole tasks.

TABLE I
POSITIONING ERROR IN TELEOPERATION UNDER FULL OPERATOR DIRECT POSITION CONTROL FOR THE TASK OF PICKING AN OBJECT AND PLACING IT ON A TARGET. POSITIONING ERRORS ARE DIFFERENCES BETWEEN THE FINAL OBJECT CORNER POSITION AND EDGE ORIENTATION FROM THE SPECIFIED TARGET CORNER POSITION AND EDGE ORIENTATION, RESPECTIVELY

	Positioning Error		
Test	*X* (mm)	*Y* (mm)	*Z* rotation (deg)
1	-5.0	+2.0	+4.0
2	+3.0	-3.0	+6.0
3	-1.5	+5.5	-4.5
4	-5.5	+1.0	+0.5
5	+3.0	+2.5	+4.0
6	-1.0	-5.5	+2.0
7	+3.5	-3.0	+0.5
8	-2.0	-1.0	-2.0
9	-7.5	+3.5	+5.0
10	-6.0	+7.0	+2.5
Mean absolute error	**3.8**	**3.4**	**3.1**
SD	(2.0)	(1.9)	(1.8)

the differences between the final object corner position and edge orientation from the specified target corner position and edge orientation, respectively.

Again using the method of teleoperation under direct position control of the robot end-effector, an experiment was performed to test the ability of an operator to perform a task that was more complex and less structured than the previous test. Three different extruded-shape objects, extrusions of a circle, square, and a modified square with one side round, respectively, and a target housing three holes of the same shapes, were tossed onto a flat surface to ensure that they were randomly positioned and oriented in front of the robot manipulator. The four robot-site camera views of the robot manipulator, the objects, and three-hole target, in their starting positions are shown in Fig. 7. A peg-in-hole task was then performed sequentially for each object under full direct operator control. The clearance between the holes and the corresponding objects were: 0.46, 0.88, 0.54, and 0.60 mm, for the square, circle, modified-square across flat edges, and modified-square across flat and round edges, respectively.

For the second type of experiment, a first series of four tests was performed to determine the accuracy in positioning the gripper, under full operator control, to be centered on an object as for an object gripping task. The robot began in the starting position and the end-effector was positioned under direct operator control until the gripper was in a position to grip the object. The test was stopped and the position and orientation of the gripper was recorded at the time a gripper-close command was made. The medial position of the stationary object was also recorded.

For the second type of experiment, a second series of six tests was performed to study the teleoperation under semi-autonomous traded and shared control and to determine the accuracy of the fine positioning of the gripper using the vision-guidance system. The end-effector began in the robot starting position and the operator coarsely positioned the end-effector in front of the object under semi-autonomous traded control beginning with operator control. The operator then transferred control to the robot and vision-guidance system by a transfer-control command. Fine positioning of the end-effector was then carried out by the robot and vision-guidance system to align and centre the gripper with the object, as explained in Section V-B-2 and Fig. 6. After the fine positioning, the operator was able to position the end-effector under shared control to approach the object and close the gripper to grip the object. The test was completed when control of the end-effector was automatically returned to the operator, 5 s after the close-gripper command. During the tests, the operator intentionally misaligned the gripper by an end-effector roll rotation about the tool axis X', to test the ability of the vision-guidance system to align the gripper with the object.

VII. RESULTS

The results of the first experiment of object placement under operator direct position control of the robot end-effector are shown in Table I. Positioning errors for the ten tests ranged from -7.5 to $+3.5$ mm in X, -5.5 to $+7.0$ mm in Y, from the two specified target edges, respectively. The mean absolute errors were very low, 3.8 mm in X and 3.4 mm in Y with standard deviations (SDs) of 2.0 mm and 1.9 mm, respectively. The error in rotation of the object with respect to the target (Z rotation) ranged from $-4.5°$ to $+6.0°$ with a mean absolute error of $3.1°$ and SD $1.8°$. The results in positioning are rather excellent, especially considering the small size of the object and target in the camera images used for feedback [Fig. 4(b)]. However, some minor correction of the end-effector position and orientation for overshoot was required during the object manipulation tasks, mainly preceding a gripper closing to pick the object and gripper opening to place it on the target. This can be seen in Fig. 8, where the position and orientation of the end-effector (tool-control point) and operator hand for a typical test (Test 5) are shown. The 3-D end-effector and operator hand paths for the entire test [Fig. 8(a)] and for the period from close gripper to open gripper [Fig. 8(b)] are shown, as well as the gripper and hand X, Y, Z displacements [Fig. 8(c)–(e)] and rotations [Fig. 8(f)–(h)]. Corrections in positioning associated with a lag of the end-effector behind the hand are seen from time 10 to 30 s

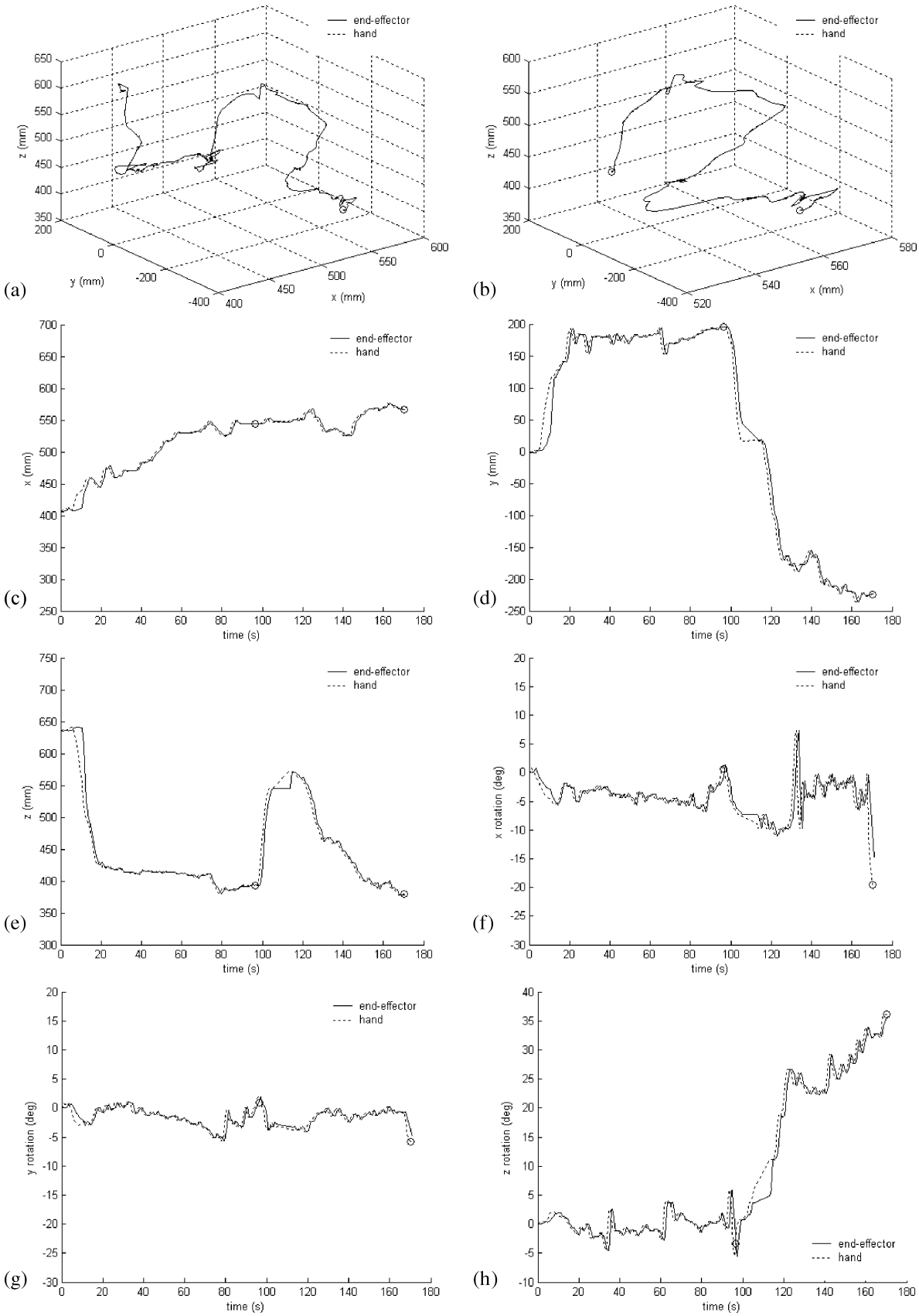

Fig. 8. Position and orientation of the robot end-effector and operator hand during the first teleoperation experiment of picking an object and placing it on a target under full operator direct position control showing (a) 3-D paths for the entire test, (b) 3-D paths for the period from closed gripper to open gripper, displacement in (c) X, (d) Y, and (e) Z, and rotations about (f) X, (g) Y, and (h) Z. Gripper closing and gripper opening are both indicated by the symbol "O" in each graph.

in Fig. 8(c)–(h). The high lag may have been partly due to the redundancy of the elbow and tool-roll rotations in the starting position, where the robot end-effector would adjust its position and orientation before executing any further motion. Lag during the entire test was also due to the time delay between acquisition of hand images to execution of robot motion. This time delay is due to the image processing in the hand-marker tracking; transfer of 2-D hand-position data between the operator-tracking and robot-site computers; data processing at the robot-site computer (reconstruction of 3-D human-hand positions and orientations from 2-D hand-position data, computation of desired robot positions and orientations from 3-D hand positions, and analyzing hand-marker position data for commands based on hand open/close); communication between the robot-site computer and robot controller; and robot execution of the motion instructed to it. The highest time delays are due to the image processing and robot-motion execution. Before closing the gripper to pick up the object during the period 30–95 s (closing indicated by a small circle in the graph), the operator made three adjustments of approximately $\pm 5^\circ$ in yaw Z rotation [Fig. 8(h)] as well as smaller corrections to align the gripper with the object. Part of the adjustment was due to the closing gripper command itself, which required the thumb and index fingers to move toward each other. This inadvertently caused yaw rotation of the hand. Smaller adjustments were made in pitch Y rotation [Fig. 8(g)] and X roll rotation [Fig. 8(f)] during the period 80–95 s, and in X displacement [Fig. 8(c)] 75–90 s. The larger errors in Y and Z translation, and X and Z rotation [Fig. 8(d)–(f) and (h), respectively) from 100 to 120 s, are due to robot end-effector adjustments mainly in Z rotation [Fig. 8(h)] and resulting Y translation [Fig. 8(d)], while Z translation [Fig. 8(e)] and X rotation [Fig. 8(f)] were constant. These adjustments occurred due to the kinematic redundancy in elbow and tool-roll rotation, which required the robot to choose the best configuration before continuing with the next instructed motion. This occurred as the end-effector was midway in translating from the object starting position $(+Y)$ to the target position $(-Y)$, at the instant the end-effector passed across the robot starting position in Y. The operator ceased Y translation during this period. In placing the object on the target, adjustments were made mainly in Y displacement [Fig. 8(d)], roll X rotation [Fig. 8(f)], and yaw Z rotation [Fig. 8(h)], from 130 to 170 s.

Again using direct position control, the operator was able to perform the peg-in-hole task with the extruded circle and square; however, some correction of the initial object placement was used for both objects, by touching the top and side of the objects by teleoperation. The operator was able to place the modified-square object in the corresponding hole; however, the part was incorrectly oriented and this could not be corrected simply. The final positions of the target, objects, and end-effector at the end of the experiment are shown in Fig. 9. Some movement of the three-hole target from its starting position can be seen.

Positioning errors after end-effector alignment by the operator and after alignment by the robot-vision system are shown in Tables II and III, respectively. Mean absolute errors in centering the gripper on the object (Y) were lower when carried out under control of the robot-vision system, 4.5 mm

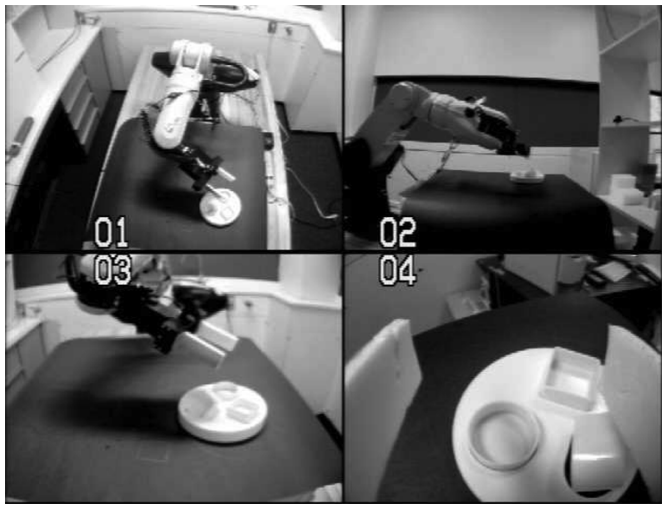

Fig. 9. Four robot-site camera views of the robot manipulator, the extruded-shape objects, and three-hole target, at the end of the peg-in-hole experiment.

(Table III) compared to those when under operator control, 13.8 mm (Table II). The fine adjustment of the tool-roll orientation to align the gripper with the object under robot-vision-system control had a lower mean absolute error of 2.5° (Table III) compared to 4.6° (Table II) under operator control. These results suggest a significant advantage in using the semi-autonomous traded and shared control with the robot vision-guidance system compared to full operator direct control. The pitch Y and yaw Z rotations were performed under operator control in both the operator direct control and semi-autonomous control tests. The mean absolute error in yaw Z rotation of 3.1° for the semi-autonomous control test (Table III) was low compared to 7.7° for the operator full control test (Table II). This may mainly have been due to the yaw rotation being locked under shared control (after tool-roll alignment was completed) while the operator controlled the end-effector approach toward the object. The operator may also have performed better in controlling the Z rotation just before transferring control to the robot-vision system for the semi-autonomous case, because of the reduced burden controlling less degrees of freedom, knowing that the centering and tool roll would be corrected by the robot-vision system.

Fig. 10 shows the position and orientation of the end-effector and operator hand for a typical test (Test 6) under semi-autonomous traded and shared control. The 3-D end-effector and operator hand paths for the entire test [Fig. 10(a)] and for the period from transfer-control-to-robot to transfer-control-to-operator [Fig. 10(b)] are shown, as well as the gripper and hand X, Y, Z displacements [Fig. 10(c)–(e)] and rotations [Fig. 10(f)–(h)]. The major positioning adjustments by the operator were preceding the transfer of control from the operator to the robot-vision system, indicated by the first asterisk $(^*)$, from approximately 15 to 65 s in Y translation [Fig. 10(d)], X and Z rotation (Fig. 10(f) and (h), respectively), and to a lesser extent in Y rotation [Fig. 10(g)]. The adjustment in Z rotation appears slightly prolonged due to the closing of hand by the index finger and thumb. The end-effector centering (Y translation), and roll alignment (X rotation) under robot

TABLE II
POSITIONING ERROR WHEN CLOSING GRIPPER TO GRIP OBJECT IN TELEOPERATION UNDER OPERATOR FULL CONTROL

	Positioning Error When Closing Gripper			
Test	*Y* (mm)	Roll : *X* rotation (deg)	Pitch : *Y* rotation (deg)	Yaw : *Z* rotation (deg)
1	+23	+2.0	-1.2	-12.0
2	+7.5	+2.0	+3.5	-8.2
3	-10.6	+2.5	+3.0	+3.6
4	+14	+11.8	-2.7	-7.1
Mean absolute error	**13.8**	**4.6**	**2.6**	**7.7**
SD	(5.8)	(4.2)	(0.9)	(3.0)

TABLE III
POSITIONING ERROR WHEN CLOSING GRIPPER IN TELEOPERATION UNDER SEMI-AUTONOMOUS TRADED AND SHARED CONTROL

	Positioning Error When Closing Gripper			
Test	*Y* (mm)	Roll : *X* rotation (deg)	Pitch : *Y* rotation (deg)	Yaw: *Z* rotation (deg)
1	+4.7	+2.8	0.6	-2.9
2	+1.0	+2.5	-5.9	-1.1
3	+0.1	+2.6	-1.2	-0.9
4	+4.2	+1.7	-6.7	-3.0
5	+8.2	+2.3	-1.6	-6.0
6	+8.6	+3.0	-6.4	-4.7
Mean absolute error	**4.5**	**2.5**	**3.7**	**3.1**
SD	(3.2)	(0.4)	2.6	(1.8)

vision-system control are seen in Fig. 10(d) and (f), from approximately 80 to 90 s. This was followed by shared control between the operator and robot, with the operator controlling the approach toward the object [Fig. 10(c)] from 95 to 125 s, then gripper closing indicated by the circle, and finally return of full control to the operator, indicated by the second asterisk at the end of the task. The locked yaw Z rotation of the robot during the approach to the object, described earlier, can be seen in Fig. 10(h), along with the locked Y rotation [Fig. 10(g)], from 75 s until control is returned to the operator, indicated by the second asterisk at the end of the task several seconds after the gripper closing. The large offset in hand and end-effector positions and rotations starting just before the first transfer of control, is due to hand motion that occurred during execution of the transfer-control command using the repeated hand close–open sequence. This hand motion is ignored and the offset does not affect the robot motion, as the reference hand positions and rotations are updated during the centering and alignment under robot-vision system control. This ensures that the end-effector can follow the new hand motion when control is returned to the operator, without requiring the operator to follow the robot motion.

VIII. DISCUSSION

In robot teleoperation in a remote unstructured environment, it is assumed that all remote-robot site components, including the robot manipulator, robot controller, end-effector camera, and other cameras, could be mounted on a mobile platform that would enter the unstructured environment. The presented method of robot teleoperation was demonstrated for object gripping, picking, and placement on a fixed target, and for fine positioning for gripping under semi-autonomous traded and shared control. One advantage of the system is the inclusion of a human in the control loop for decision making. This allows an object to be grasped, taken, moved, and placed without any prior knowledge of its starting location and even target location. Such tasks could also be done for multiple objects in the environment where decision-making is required for the object and target selection, with applications in sorting and clean up, which may involve hazardous materials. It is expected that the system could be used for more complex robot motions within the robot-joint limits. Peg-in-hole tasks were also demonstrated with randomly-positioned and oriented extruded-shape objects and target holes. For tasks such as assembly and disassembly that involve more constrained peg-in-hole tasks than demonstrated here, compliance in the gripper fingers, greater peg-hole clearance, and chamfers may be required unless force feedback could be included in the system.

The human–robot teleoperation system would permit grabbing objects that are moving with unknown or random motion, and placing them on targets that are also moving, as long as the motion is slow. Applications include inspection, selection and rejection of objects, ranging from manufactured parts and food, to hazardous materials. More generally, any task that involves end-effector motion along a previously undetermined path, determined by the human in real-time during teleoperation, could be achieved. This includes painting and exploration. An exploration task would involve manipulation of objects that would be newly exposed, where their shape would be unknown.

In order to grip an object of unknown shape using shared control, the vision-guidance system would have to be further developed. Currently, the intelligence incorporated for shared-control teleoperation includes: determination of the intended direction of motion of the operator in gripping an object, determination of the operator's desire to take back full control of the robot or grip an object, and reduction of the risk of collision when the end-effector is approaching the object.

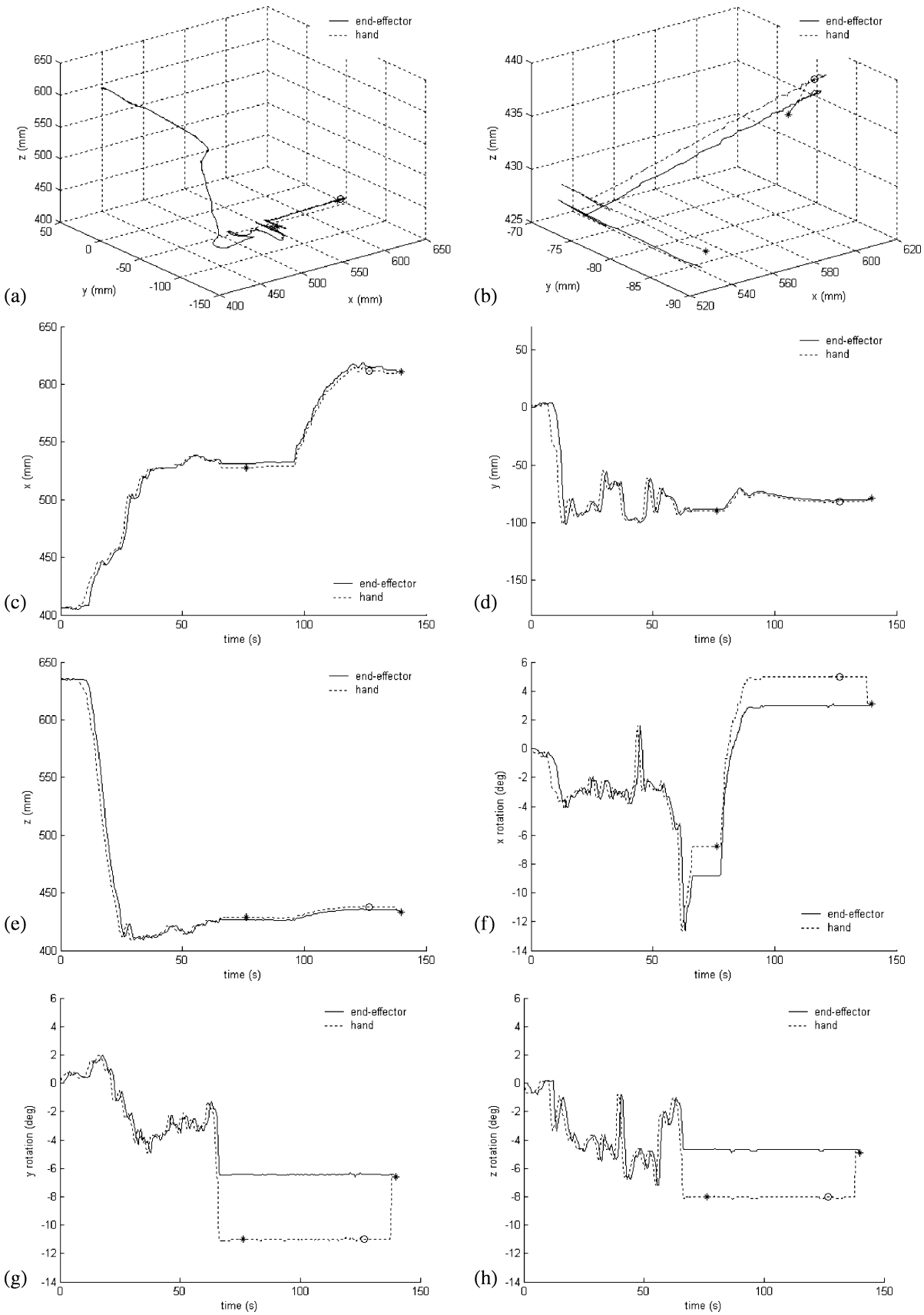

Fig. 10. Position and orientation of the robot end-effector and operator hand during teleoperation under semi-autonomous traded and shared control: (a) 3-D paths for the entire test, (b) 3-D paths for the period from transfer-control-to-robot to transfer-control-to-operator; displacement in: (c) X, (d) Y, and (e) Z, and rotations about (f) X, (g) Y, and (h) Z. Transfer control from operator to robot and transfer control from robot to operator are both indicated by the symbol "$*$" in each graph, and a gripper closing is indicated by the symbol "O."

For more complex tasks such as operating in an environment of multiple objects, segmentation of the object or objects of interest may be more complicated. For moving objects, path prediction based on the human operator's hand motion may be used, or alternatively, tracking of the moving object by the end-effector mounted camera or other robot-site cameras could be developed. Intelligence to avoid obstacles may also be necessary. The use of stereo cameras and range cameras to reconstruct the robot environment in 3-D would aid in such complex tasks.

The robot-vision system currently has the intelligence for handling rectangular prismatic objects. Under traded control, the robot-vision system is currently intelligent to determine accurately where the object of interest is in the 2-D image, once the operator has placed the end-effector, and thus the camera, such that the object appearing closest to the center of the image is the one of interest. The presence of an object can be determined even if the object is not fully visible in the image. The robot-vision system also has the intelligence to determine that the desired orientation of the gripper in order to permit gripping is across the object's width. In further research, the motion of the operator's hand mainly along a straight line, would be used to indicate the intention of the operator to approach and grip an object.

This paper is a significant contribution to vision-based and vision-guidance based teleoperation systems. By using vision-based tracking, the present method of robot-manipulator teleoperation permits communication of tasks to the robot manipulator in a natural manner, generally using the same hand motions that would normally be used for a task. The vision-based tracking is noncontacting, and is therefore less hindering of hand motion compared to the use of exoskeletal [1] and sensor-based devices [2]–[6], the most common being the Data Glove [13]. The proposed method allows the user to concentrate on the entire task at hand rather than having to think of basic commands that the teleoperation system understands, as with voice-recognition-based teleoperation systems [13]. The method in this paper is also more flexible than approaches that use scripts of pre-programmed tasks which require knowledge of objects to be manipulated and the working environment [13]. The flexibility of the present method would be more adaptable than these approaches in unstructured environments, where the position and orientation of objects is not known in advance. While the presented system permits simultaneous motion in six degrees of freedom, other vision-based teleoperation systems have operated with a limited number of degrees of freedom simultaneously [9], [10]. In the use of vision guidance for semi-autonomous teleoperation, the present method has more flexibility than other approaches that require comparison of real-time measured features to pre-taught image features in 2-D images [13]. The present method uses the coarse-positioning capability of the operator to initiate a fine gripper positioning and alignment on an object, without restriction on the object's position and orientation.

As the use of only two cameras to track the human-hand markers limited the permitted operator hand motion, ongoing and further research will include the use of more cameras to permit greater hand motion, and markerless hand tracking. The use of semi-autonomous traded and shared control employing the robot vision-guidance system was advantageous for fine positioning of the end-effector in object gripping tasks. Currently the end-effector camera (Camera 4) is not able to provide a view of the target for object placement tasks. Future research will include alternative end-effector-camera mounting to permit robot-vision guidance in object placement. An alternative method of transferring control between operator and robot, such as voice control, will be employed, to eliminate the extra yaw Z adjustment that was required by the operator during a repeated hand close–open sequence when executing a transfer-control command. This will make the robot control more natural, and leave the closing and opening hand actions performed by the operator as natural ones to perform only the closing and opening of the gripper.

IX. Conclusion

Teleoperation of a robot manipulator was carried out using a noncontacting vision-based human–robot interface that permitted the operator to communicate pick-and-place motion tasks to the robot, using simultaneous hand motion in six degrees of freedom. Under operator direct position control of the robot end-effector, the operator was able to achieve a high accuracy in placing an object on a target. Operator correction of the end-effector position and orientation during object manipulation tasks occurred mainly preceding a gripper closing and gripper opening. This was likely due to the small size of the object and target in the camera images used for feedback, and delay between hand-image acquisition and robot motion execution. Semi-autonomous traded and shared control aided in achieving a more accurate positioning and orientation of the end-effector for object gripping tasks, and were an advantage over operator direct position control. This occurred even for motions controlled by the operator, probably because of the reduced burden in controlling several axes of motion simultaneously. Alternative end-effector-camera mounting for close-range visual feedback will be used in future research to permit a similar advantage of robot-vision guidance in object placement. Some adjustment of the end-effector yaw rotation was required of the operator when effecting a transfer of control command, because of the motion of the thumb and index finger markers in repeated hand closing. Alternative methods of transferring control, such as voice control, will be considered in future work.

Acknowledgment

The research reported in this paper was carried out at the Human-Machine Interfaces and Intelligent Systems Laboratory, Department of Mechanical Engineering, University of Ottawa, Ottawa, ON, Canada.

References

[1] S. Chang, J. Kim, I. Kim, J. H. Borm, and C. Lee, "KIST teleoperation system for humanoid robot," in *Proc. 1999 IEEE/RSJ Int. Conf. Intelligent Robots and Systems*, 1999, pp. 1198–1203.

[2] T. Harada, T. Sato, and T. Mori, "Human motion tracking system based on skeleton and surface integration model using pressure sensors distribution bed," in *Proc. Workshop Human Motion (HUMO'00)*, 2000, pp. 99–106.

[3] T. Tezuka, A. Goto, K. Kashiwa, H. Yoshikawa, and R. Kawano, "A study on space interface for teleoperation system," in *Proc. IEEE Int. Workshop Robot and Human Communication*, 1994, pp. 62–67.
[4] E. R. Bachmann, R. B. McGhee, X. Yun, and M. J. Zyda, "Inertial and magnetic posture tracking for inserting humans into networked virtual environments," in *Proc. ACM Symp. Virtual Reality Software and Technology (VRST)*, Banff, AB, Canada, 2001, pp. 9–16.
[5] C. Verplaetse, "Inertial proprioceptive devices: self-motion-sensing toys and tools," *IBM Syst. J.*, vol. 35, no. 3, pp. 639–650, 1966.
[6] O. Fukuda, T. Tsuji, M. Kaneko, and A. Otsuka, "A human-assisting manipulator teleoperated by EMG signals and arm motions," *IEEE Trans Robot. Autom.*, vol. 19, no. 2, pp. 210–222, Apr. 2003.
[7] J. Cui, S. Tosunoglu, R. Roberts, C. Moore, and D. W. Repperger, "A review of teleoperation system control," in *Proc. Florida Conf. Recent Advances in Robotics, FCRAR*, Boca Raton, FL, 2003, pp. 1–12.
[8] C. Hu, M. Q. Meng, P. X. Liu, and X. Wang, "Visual gesture recognition for human-machine interface of robot teleoperation," in *Proc 2003 IEEE/RSJ Int. Conf. Intelligent Robots and Systems*, Las Vegas, NV, Oct. 2003, pp. 1560–1565.
[9] T. Kurpjuhn, K. Nickels, A. Hauck, and S. Hutchinson, "Development of a visual space-mouse," in *Proc. Int. Conf. Robotics and Automation (ICRA)*, 1999, pp. 3230–3235.
[10] F. Lathuilière and J. Y. Hervé, "Visual hand posture tracking in a gripper guiding application," in *Proc. Int. Conf. Robotics and Automation (ICRA)*, 2000, pp. 1688–1694.
[11] Y. I. Abdel-Aziz and H. M. Karara, "Direct linear transformation from comparator coordinates into object space coordinates in close-range photogrammetry," in *Proc. Symp. Close-Range Photogrammetry*, Urbana, IL, 1971, pp. 1–18.
[12] Y. S. Park, "Structured beam projection for semi-automatic teleoperation," in *Proc SPIE, Optomechatronic Systems*, vol. 4190, 2001, pp. 192–201.
[13] C. Martens, N. Ruchel, O. Lang, O. Ivlev, and A. Gräser, "A FRIEND for assisting handicapped people," *IEEE Robot. Autom. Mag.*, vol. 8, no. 1, pp. 57–65, Mar. 2001.

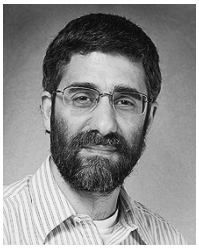

Jonathan Kofman (M'97) received the B.Eng. degree from McGill University, Montréal, QC, Canada, in 1982, the M.A.Sc. degree from the Ecole Polytechnique, Montréal, QC, Canada, in 1987, and the Ph.D. degree from the University of Western Ontario, London, ON, Canada, in 2000, all in mechanical engineering.

From 1983 to1984 and 1987 to 1995, he was a Research Engineer working in the biomedical and rehabilitation areas. From 1987 to 1991, his research in Jönköping, Sweden, included development of laser-camera range sensors and CAD/CAM systems for prosthetics, which were commercialized by CAPOD Systems AB, Sweden, in 1991. In his later research, a technique for unconstrained range sensing was awarded a U.S. patent. From 2000 to 2004, he was an Assistant Professor in the Department of Mechanical Engineering, University of Ottawa, where he founded and directed the Human-Machine Interfaces and Intelligent Systems Laboratory. He is currently an Assistant Professor in the Department of Systems Design Engineering, University of Waterloo, Waterloo, ON, Canada. His research interests include human–machine interfaces, telerobotics, range-sensing and optical-sensor design, computer vision, biomechatronic and optomechatronic intelligent systems, and biomedical applications.

Dr. Kofman is a Member of the IEEE Robotics and Automation and IEEE Engineering in Medicine and Biology Societies, as well as the International Society for Optical Engineering (SPIE), and American Society of Biomechanics, and he holds licenses from the Professional Engineers of Ontario and Ordre des Ingénieurs du Québec. He has recently coauthored three international conference award papers.

Xianghai Wu was born in Sichuan, China, in 1972. He received the B.S. degree in electronics engineering from Beijing University of Aeronautics and Astronautics, Beijing, China, in 1995, and the M.S. degree in aerospace engineering from the Chinese Academy of Space Technology, Beijing, China, in 1998. He is currently working toward the Ph.D. degree in the Department of Systems Design Engineering, University of Waterloo, Waterloo, ON, Canada.

From 1998 to 2000, he was a System Engineer at the Beijing Institute of Control Engineering. He then worked in the information technology industry for one year. His research interests include computer vision, robotics, teleoperation, and visual servoing.

Mr. Wu is a Student Member of the International Society for Optical Engineering (SPIE) and was awarded the Best Student Paper Award at the conference *Machine Vision and its Optomechatronic Applications* at SPIE Optics East, 2004.

Timothy J. Luu was born in Abbotsford, BC, Canada, in 1980. He received the Bachelor of Applied Science degree in engineering physics, specializing in mechanical engineering, from the University of British Columbia, Vancouver, BC, Canada, in 2003. He is currently working toward the Master of Applied Science degree in mechanical engineering at Carleton University, Ottawa, ON, Canada,

He was previously involved in prototype development at QuestAir Technologies, active noise control research at the University of British Columbia, and automated process monitoring of laser welding and cutting at Laser Zentrum Hannover, all as summer positions. He has also developed prototypes for Ballard Power Systems and The Pulp and Paper Research Institute of Canada as sponsored projects. He is currently a Research Assistant at Carleton University, developing a means to integrate type and approximate dimensional synthesis of four-bar planar linkages for rigid-body guidance. His research interests include automation, control, robotics, mechatronics, and kinematic synthesis of planar mechanisms.

Siddharth Verma was born in New Delhi, India. He received the B.Sc.(Engg.) degree from Dayalbagh Educational Institute, Dayalbagh, India, in 2000, and the M.A.Sc. degree from the University of Ottawa, Ottawa, ON, Canada, in 2003, both in mechanical engineering. He is currently working toward the Ph.D. degree in mechanical engineering at McGill University, Montréal, QC, Canada.

He was a Mechanical Engineer for a year at TATA Motors in India after receiving the B.Sc.(Engg.) degree. His research has been concentrated on computer vision, image processing, robotics, telerobotics, and dynamics. He is currently working in the area of on-orbital satellite servicing, concentrating on developing a technique for autonomous capture and inertial properties estimation of a non-cooperating satellite using 3-D vision sensors mounted on a robot.